

# Quantum dynamics in splitting a harmonically trapped Bose-Einstein condensate by an optical lattice: Truncated Wigner approximation

L. Isella<sup>1</sup> and J. Ruostekoski<sup>2</sup>

<sup>1</sup>*European Commission, Joint Research Centre, I-21020 Ispra (Va), Italy*

<sup>2</sup>*School of Mathematics, University of Southampton, Southampton, SO17 1BJ, UK*

(Dated: August 20, 2018)

We study the splitting of a harmonically trapped atomic Bose-Einstein condensate when we continuously turn up an optical lattice (or a double-well) potential. As the lattice height is increased, quantum fluctuations of atoms are enhanced. The resulting nonequilibrium dynamics of the fragmentation process of the condensate, the loss of the phase coherence of atoms along the lattice, and the reduced atom number fluctuations in individual lattice sites are stochastically studied within the truncated Wigner approximation. We perform a detailed study of the effects of temperature and lattice height on atom dynamics, and investigate the validity of the classical Gross-Pitaevskii equation in optical lattices. We find the atom number squeezing to saturate in deep lattices due to nonadiabaticity in turning up of the lattice potential that is challenging to avoid in experiments when the occupation number of the lattice sites is large, making it difficult to produce strongly number squeezed (or the Mott insulator) states with large filling factors. We also investigate some general numerical properties of the truncated Wigner approximation.

PACS numbers: 03.75.Lm,03.75.Kk,03.75.Gg

## I. INTRODUCTION

The experimental progress in loading ultra-cold atomic gases in weakly coupled mesoscopic traps formed by periodic optical potentials has provided a dilute atomic system with strongly enhanced interactions. Examples of this progress include experiments on the Bose-Einstein condensate (BEC) coherence [1–5], the atom number-squeezed states [6], the Mott insulator (MI) phase transition [7–11], atom dynamics [11–15], and fermionic systems [16–18]. Ultra-cold atoms trapped in an optical lattice resemble traditional condensed matter crystal lattice systems [19], but optical lattices are amenable to much higher experimental control. The lattice strength can be easily modified [2, 6–9, 20] and it could be possible to engineer, e.g., complex lattice geometries [21], interatomic interactions [22, 23], and the spatial profiles of the atomic hopping amplitude between the lattice sites [24–29].

In order to produce atomic lattice systems close to their ground state, atoms need to be adiabatically loaded into the optical lattices by continuously turning up the lattice potential. The BEC is initially confined in a harmonic trap. The increasing strength of the lattice potential reduces the tunneling amplitude between the neighboring lattice sites and the system becomes more strongly interacting. The strong interactions enhance quantum fluctuations, eventually destroying the long-range phase coherence of the atoms and fragmenting the BEC. If the turning-up of the lattice potential is not adiabatic, the quantum fluctuations of the atoms can be far from their ground state properties, resulting in complex dynamics.

In order to preserve adiabaticity during the turning-up of the optical lattice potential, the rate of change of the Hamiltonian has to be slower than any time scale of the system. The required slow ramping-up time generally makes it very difficult to reach the MI ground

state experimentally, when there are many atoms per lattice site, as we demonstrated in Ref. [30]. The situation is different from the MI state experiments [7–11] with small filling factors, because of rapidly emerging energy gap and larger quantum fluctuations in the case of small atom numbers. The nonadiabaticity of the turning up of the optical lattice has recently been theoretically studied also by using classical Gross-Pitaevskii equation (GPE) (without thermal and quantum fluctuations): The buildup of an inhomogeneous phase profile [31, 32] was identified in the classical analysis as a potential signature for nonadiabaticity.

In this paper we study matter wave dynamics beyond the classical mean-field theory by considering a harmonically trapped BEC that is dynamically split by an optical lattice potential. In our numerical model the quantum and thermal fluctuations of the atoms are included in a classical stochastic field description within the truncated Wigner approximation (TWA). We provide a more detailed and extended analysis of our previous results [30] by also studying the limits of validity of the classical GPE and the general numerical properties of the TWA. The lattice systems we consider have large occupation numbers per site. Recent experimental studies by Orzel *et al.* [6] on the squeezing of atom number fluctuations have been performed in the similar limit of strong optical lattices and large filling factors. The states with squeezed atom number fluctuations with high occupation numbers are of great interest in precision measurements, as they may allow Heisenberg limited interferometry with potential technological applications [33].

We study the nonequilibrium dynamics of the BEC that is split by the lattice potential, describing the loss of phase coherence along the lattice, the atom number fluctuations within individual lattice sites, and the fragmentation process of the BEC. We show in numerical TWA

simulations how the atom number fluctuations evolve in time after the turning up of the lattice potential from almost Poisson initial value to a strongly reduced result that depends on the parameters of the system. We also show that the squeezing of atom number fluctuations saturates for deep lattices, as a consequence of nonadiabatic turning up of the lattice potential. The saturation of the number squeezing for deep lattices was experimentally observed in Ref. [6]. This system was not tightly elongated as our 1D numerical model, but we can still make qualitative comparisons to the experimental data. Although the saturation was assumed in Ref. [6] to be an artifact of the analysis method of the interference measurement, we also numerically find a similar saturation effect in a qualitative agreement with the experiment. Since the atom number fluctuations in Ref. [6] were indirectly detected from the phase noise of the interference measurement, not all the experimentally detected phase fluctuations may have directly corresponded to the atom number squeezing, due to the possibility of nonadiabatic loading of the atoms. We find, however, in the TWA simulations that considerable atom number squeezing can be present even in the nonadiabatic regime in the presence of increased phase noise and a nonuniform phase profile.

In the numerical TWA simulations we first consider a BEC that is split by a simple double-well potential and compare the numerical results to the phase collapse rate calculated for an equilibrium BEC in a double-well potential. We then apply the TWA to the splitting of a BEC by a periodic optical lattice potential that constitutes the main results of the paper. We evaluate the dynamics of the phase coherence between atoms occupying different lattice sites and the atom number fluctuations in individual sites during and after the splitting of the BEC. We study in detail different cases when we vary the final height of the lattice potential, the initial temperature and nonlinearity. In order to investigate the limits of validity of the classical GPE, we also systematically compare the TWA simulation results to the GPE results by varying the initial temperature and the final lattice height. In shallow lattices and at low temperatures the two approaches yield very similar results for the coherence properties and atom statistics. However, as the lattice height and/or the temperature are increased the validity of the GPE becomes poorer.

We also study the generation of the initial state in the TWA simulations using an ideal gas. The stochastic noise is sampled for noninteracting atoms, before turning up the nonlinearity in order to produce the initial state of an interacting system. We find that this technique works better at low temperatures in which case the results are close to the ones obtained by more accurate TWA calculations.

Since the TWA simulations return symmetrically order expectations values, we also investigate the importance of the particular stochastic representation of the density matrix. We demonstrate by numerical examples that the correct transformation between symmetric and normal

operator orderings is very crucial in obtaining the correct physical results, especially at low temperatures.

The TWA was introduced in nonlinear optics to study quantum fluctuations [34] and it has provided successful descriptions for nonlinear optical squeezing [35]. The TWA and other closely related classical field methods [30, 36–46] have previously also been applied to the studies of atomic BEC dynamics. In our earlier studies [30, 43] we found that the TWA is particularly useful to study bosonic atom dynamics in optical lattices in the limit where the full multi-mode dynamics, beyond the tight-binding approximation, becomes important and when the atom filling factor in the lattice is large. In Ref. [43] the TWA was able to describe the experimentally observed dissipative atom dynamics in tightly confined, shallow 1D optical lattices [11] even in a strongly fluctuating quantum system.

In Sec. II we introduce the TWA and the methods to extract the normally ordered physical observables in the numerical simulations. We also describe the general numerical approach used in the TWA simulations in Sec. II C. The splitting of a harmonically trapped BEC by an optical potential is studied in Sec. III. We first consider a double-well potential in Sec. III A and an optical lattice with a small number of sites in Sec. III B. The main numerical results of the paper are presented in Sec. III C where we address an optical lattice with a larger number of sites. The effects of the final lattice height on the atom number fluctuations and matter wave coherence are studied in Sec. III C 1. We analyze the adiabaticity of the turning up of the lattice potential and present qualitative comparisons to the experiment of Ref. [6]. The effects of initial temperature and nonlinearity on the dynamics are studied in Sec. III C 2. We compare the TWA simulation results to the classical GPE results in Sec. III C 3 by varying the initial temperature and the final lattice height. The change of temperature during the splitting is analyzed in Sec. III C 4. An alternative method for generating the initial state of the TWA simulations by turning up the nonlinearity is studied in Sec. III C 5. In Sec. III C 6 we consider the effect of the initial state noise sampling in the TWA and in Sec. III C 7 the importance of symmetric operator ordering in the Wigner representation. A few concluding remarks are made in Sec. IV. The Bogoliubov approximation in a discrete tight-binding approximation is introduced in Appendix A and the three-body losses are estimated in Appendix B.

## II. OVERVIEW OF THE METHOD

### A. Truncated Wigner approximation

We assume that the bosonic atoms are trapped in a tight elongated (along the  $x$  direction) cigar-shaped (prolate) trap  $V_{3D}(x, y, z) = m[\omega^2 x^2 + \omega_{\perp}^2 (y^2 + z^2)]/2$ , with the trap frequencies satisfying  $\omega \equiv \omega_x \ll \omega_{\perp} \equiv \omega_y = \omega_z$ .

Here the radial frequency is denoted by  $\omega_\perp$  and the axial frequency by  $\omega$ . We ignore the density fluctuations along the transverse directions in order to obtain an effective 1D Hamiltonian:

$$\hat{H} = \int dx \hat{\psi}^\dagger(x) \hat{\mathcal{L}} \hat{\psi}(x) + \frac{g_{1D}}{2} \int dx \hat{\psi}^\dagger(x) \hat{\psi}^\dagger(x) \hat{\psi}(x) \hat{\psi}(x). \quad (1)$$

Here

$$\hat{\mathcal{L}} \equiv \hat{T} + V_h(x) + V_o(x, t) - \mu, \quad (2)$$

includes the kinetic energy  $\hat{T} \equiv -\hbar^2 \partial_x^2 / (2m)$ , the harmonic trapping potential along the axial direction  $V_h \equiv m\omega^2 x^2 / 2$ , and the time-dependent periodic optical lattice potential, or in the case of the double-well a Gaussian potential barrier,  $V_o(x, t)$ . The atom mass and the chemical potential are denoted by  $m$  and  $\mu$ , respectively. The effective 1D interaction strength is given by  $g_{1D} = 2\hbar\omega_\perp a$ , where  $a$  is the scattering length.

We study the dynamics of a finite-temperature BEC within the TWA when we load the atoms into an optical lattice by ramping up the periodic lattice potential. The TWA may be obtained by using the familiar techniques of quantum optics [47, 48] to derive a generalized Fokker-Planck equation for the Wigner distribution of the trapped multi-mode BEC [36]. We obtain from the Hamiltonian (1):

$$\frac{\partial W(\psi, \psi^*)}{\partial t} = \int_{-\infty}^{\infty} dx i \left\{ \frac{\delta}{\delta \psi} \left[ \left( \hat{\mathcal{L}} + g_{1D}(|\psi|^2 - 1) \right) \psi \right] - \frac{1}{4} \frac{\delta^3}{\delta^2 \psi \delta \psi^*} \psi \right\} W(\psi, \psi^*) + \text{c.c.} \quad (3)$$

Here the density operator of the quantum system is represented by a classical quasidistribution function  $W(\psi, \psi^*)$  of the complex functions  $(\psi, \psi^*)$  that correspond to the field operators  $(\hat{\psi}, \hat{\psi}^\dagger)$ . The expectation values in the Wigner representation  $\langle \dots \rangle_W$  are obtained from the quasidistribution function:

$$\langle \psi^*(x_1) \dots \psi^*(x_k) \psi(x_{k+1}) \dots \psi(x_l) \rangle_W = \int d^2\psi W(\psi, \psi^*) \psi^*(x_1) \dots \psi^*(x_k) \psi(x_{k+1}) \dots \psi(x_l). \quad (4)$$

The expectation values obtained according to the Wigner distribution correspond to the expectation values of quantum operators that are in symmetric, or Weyl, order.

The diffusion matrix of the Fokker-Planck equation (3) for  $W(\psi, \psi^*)$  vanishes identically and the dynamical quantum noise acts via third-order derivatives. It is useful to write Eq. (3) in terms of stochastic differential equations for  $(\psi, \psi^*)$  whose ensemble average of the dynamics generates the expectation values (4) obtained

from the quasidistribution function. The TWA consists of neglecting the third-order derivatives in Eq. (3), resulting in a deterministic equation for the classical field  $\psi_W$  which coincides with the Gross-Pitaevskii equation (GPE) [36]:

$$i\hbar \frac{\partial \psi_W(x, t)}{\partial t} = \left[ \hat{\mathcal{L}} + g_{1D}(|\psi_W(x, t)|^2 - 1) \right] \psi_W(x, t). \quad (5)$$

Here we have introduced a subscript in  $\psi_W$  in order to emphasize that it denotes the classical Wigner representation of the field operator. We have also explicitly included the constant phase factors from Eq. (3). Although the time evolution represented by Eq. (5) is deterministic, the thermal and quantum fluctuations are still included in the initial state of  $\psi_W$  that represents an ensemble of Wigner distributed wave functions. The neglected terms in the TWA are small when the amplitudes of the Wigner distribution are large. It should be emphasized that without ignoring the third-order derivatives in the Fokker-Planck equation no simple stochastic description exists. The stochastic representation in the TWA for the field operator exists for the states for which  $W(\psi_W, \psi_W^*)$  is positive. The stochastic description is especially useful since a single field  $\psi_W$  incorporates both the condensate and the noncondensate populations.

The atoms are initially assumed to be in thermal equilibrium in a harmonic trap, before the periodic optical lattice potential is turned up. In order to sample the initial state stochastically, we solve the quasiparticle excitations of the BEC within the Bogoliubov approximation. We expand the field operator  $\hat{\psi}(x, t=0)$  in terms of the BEC ground state amplitude  $\hat{\alpha}_0 \psi_0$ , with  $\langle \hat{\alpha}_0^\dagger \hat{\alpha}_0 \rangle = N_0$ , and the excited states:

$$\hat{\psi}(x) = \psi_0(x) \hat{\alpha}_0 + \sum_{j>0} [u_j(x) \hat{\alpha}_j - v_j^*(x) \hat{\alpha}_j^\dagger]. \quad (6)$$

Here  $\hat{\alpha}_j$  are the corresponding quasiparticle annihilation operators, with

$$\langle \hat{\alpha}_j^\dagger \hat{\alpha}_j \rangle = \bar{n}_j \equiv \frac{1}{\exp(\epsilon_j / k_B T) - 1}, \quad (7)$$

and  $\psi_0$  is ground state solution of the GPE with the chemical potential  $\mu$ . The quasiparticle mode functions  $u_j(x)$  and  $v_j(x)$  ( $j > 0$ ) and the corresponding eigenenergies  $\epsilon_j$  are obtained as solutions to the Bogoliubov equations in the subspace that is orthogonal to the ground state wave function  $\psi_0$ :

$$\begin{aligned} \left( \hat{\mathcal{L}} + 2N_0 g_{1D} |\psi_0|^2 \right) u_j - N_0 g_{1D} \psi_0^2 v_j &= \epsilon_j u_j, \\ \left( \hat{\mathcal{L}} + 2N_0 g_{1D} |\psi_0|^2 \right) v_j - N_0 g_{1D} \psi_0^{*2} u_j &= -\epsilon_j v_j. \end{aligned} \quad (8)$$

In the TWA we unravel the dynamics into individual stochastic trajectories where the classical representation  $\psi_W(x)$  of the initial state of the quantum field operator  $\hat{\psi}(x, t=0)$  in Eq. (6) is sampled according to

its Wigner distribution  $W(\psi_W, \psi_W^*)$ , so that the ensemble average of these individual realizations synthesizes the correct quantum statistical correlation functions according to Eq. (4). In particular, in order to construct  $\psi_W(x, t = 0)$  from  $\hat{\psi}(x, t = 0)$  in Eq. (6), we replace the excited state quantum operators ( $\hat{\alpha}_j, \hat{\alpha}_j^\dagger$ ) (for  $j > 0$ ) by the complex random variables ( $\alpha_j, \alpha_j^*$ ), obtained by sampling the corresponding Wigner distribution of the quasiparticles. Within the Bogoliubov approximation the operators ( $\hat{\alpha}_j, \hat{\alpha}_j^\dagger$ ) behave as a collection of ideal harmonic oscillators whose Wigner distribution in a thermal bath may be easily evaluated [48]:

$$W(\alpha_j, \alpha_j^*) = \frac{2}{\pi} \tanh(\xi_j) \exp[-2|\alpha_j|^2 \tanh(\xi_j)], \quad (9)$$

where  $\xi_j \equiv \epsilon_j/2k_B T$ . The Wigner function is Gaussian distributed with the width  $\bar{n}_j + \frac{1}{2}$ . The nonvanishing contribution to the width at  $T = 0$  for each mode represents the quantum noise. Since the Wigner function returns symmetrically ordered expectation values, we have

$$\langle \alpha_j^* \alpha_j \rangle_W = \int d^2 \alpha_j W(\alpha_j, \alpha_j^*) |\alpha_j|^2 = \bar{n}_j + \frac{1}{2}, \quad (10)$$

and similarly  $\langle \alpha_j \rangle_W = \langle \alpha_j^* \rangle_W = \langle \alpha_j^2 \rangle_W = 0$ , etc. In many realistic physical situations the number of modes required to generate the fluctuations in the initial state can significantly exceed the lowest energy band in optical lattices [43], emphasizing the multi-band nature of the TWA.

We consider large BECs with  $N_0 \gg 1$ . Since the BEC is initially weakly-interacting and confined in a harmonic trap with no optical lattice, the main contribution to the matter wave coherence is due to the thermal and quantum fluctuations of low-energy phonons that are more important than the quantum fluctuations of the initial state of the BEC mode. In most cases studied in the paper, we sample the quantum noise of the BEC mode according to the Wigner distribution of the coherent state [48]:

$$W_c(\alpha_0, \alpha_0^*) = \frac{2}{\pi} \exp\left(-2|\alpha_0 - N_0^{1/2}|^2\right), \quad (11)$$

for which  $\langle \alpha_0 \rangle_W = N_0^{1/2}$  and  $\langle \alpha_0^* \alpha_0 \rangle_W = N_0 + \frac{1}{2}$ . Since we compare the matter wave coherence between the atoms in different lattice sites, the global BEC phase is unimportant. The advantage of using the coherent state description is that the corresponding Wigner distribution is positive. As shown later in the paper, the assumption of the coherent state for the BEC mode is not very important. In fact, we could even treat the BEC mode classically without significantly affecting the results. In Section III C 6 we compare the sampling of the BEC mode according to Eq. (11) to the case in which the BEC mode is treated classically having a fixed number of atoms. A classical treatment of the ground state does not affect the prediction for the phase coherence along the lattice, but produces slightly smaller atom number fluctuations in the lattice sites.

Our TWA model for the trapped atomic vapor is for the Hamiltonian describing a closed system. In the lattice experiments the atoms are also coupled to environment, resulting in dissipation with the system relaxing towards its ground state. We could introduce a more sophisticated model, e.g., by incorporating the three-body losses and the spontaneous emission due to the lattice lasers. This would introduce also a dynamical noise term in Eq. (5). Although the spontaneous emission generates an important loss mechanism for the atoms in several experimental situations, it can be reduced by further detuning the lattice laser light from the resonance of the atomic transitions. For instance, with intense CO<sub>2</sub> lasers, that are far off-resonant, the spontaneous emission rate can be very low [49]. In Appendix B we estimate the importance of the three-body losses of atoms in a 1D optical lattice for a typical set of parameters considered in the TWA simulations.

## B. Symmetric ordering

The Wigner distribution returns symmetrically ordered expectation values for the field operators. This means that in the TWA simulations the expectation values involving the full multi-mode Wigner fields are symmetrically ordered with respect to *every* mode. In general, this can significantly complicate the analysis of the numerical results from the TWA simulations. For instance, for the initial state (6) the simple spatial correlation function in the Wigner representation would actually return:

$$\begin{aligned} \langle \psi_W^*(x) \psi_W(x') \rangle_W &= \langle \hat{\psi}^\dagger(x) \hat{\psi}(x') \rangle + \frac{N_0}{2} \psi_0^*(x) \psi_0(x') \\ &+ \frac{1}{2} \sum_{i=1} [u_i^*(x) u_i(x') + v_i(x) v_i^*(x')], \quad (12) \end{aligned}$$

where  $\langle \dots \rangle_W$  denotes the expectation value obtained from the TWA simulations and  $\langle \dots \rangle$  the normally ordered expectation value of the quantum operators. In order to extract normally ordered expectation values for the correlation functions of the BEC from the TWA simulations, Steel *et al.* in Ref. [36] defined a ‘condensate mode’ operator associated with the projection of the stochastic field onto the ground state solution. This was used to calculate the phase diffusion of a spatially static, harmonically trapped BEC. Since here we study the splitting of a BEC by a periodic optical lattice potential, it is useful to define analogously the ground state operators  $a_j$  for each individual lattice site  $j$ :

$$a_j(t) = \int_{j^{\text{th well}}} dx \psi_0^*(x, t) \psi_W(x, t), \quad (13)$$

where  $\psi_W(x, t)$  is the stochastic field, determined by Eq. (5), and  $\psi_0(x, t)$  is the ground state wave function at time  $t$ , obtained by integrating the GPE in imaginary time in the potential  $V(x, t)$ . The integration is over

one lattice site. In the following we also use the same description in a double-well potential in which case we integrate over the left and the right wells. The importance the correct operator ordering is demonstrated by a numerical example in Section III C 7.

With the projection method we can avoid the complications arising from the symmetrically ordered multi-mode field  $\psi_W$ . Using the definition in Eq. (13), the normally ordered expectation values can be easily obtained for each lattice site ground state mode  $a_j$ . For instance, the atom number in the ground state in the  $j$ th site reads:

$$n_j = \langle \hat{a}_j^\dagger \hat{a}_j \rangle = \langle a_j^* a_j \rangle_W - \frac{1}{2}, \quad (14)$$

and the atom number fluctuations in the  $j$ th site:

$$\begin{aligned} \Delta n_j &= \left[ \langle (\hat{a}_j^\dagger \hat{a}_j)^2 \rangle - \langle \hat{a}_j^\dagger \hat{a}_j \rangle^2 \right]^{1/2} \\ &= \left[ \langle (a_j^* a_j)^2 \rangle_W - \langle a_j^* a_j \rangle_W^2 - \frac{1}{4} \right]^{1/2}. \end{aligned} \quad (15)$$

Similarly, in order to characterize the phase coherence along the lattice, we may introduce the normalized first-order correlation function  $C_j$  between the atoms in the central well of the lattice and in its  $j$ th neighbor:

$$C_j = \frac{|\langle \hat{a}_0^\dagger \hat{a}_j \rangle|}{\sqrt{n_0 n_j}}. \quad (16)$$

In order to obtain directly the fluctuations in the relative phase operator  $\hat{\varphi}_{0j} \equiv \hat{\varphi}_j - \hat{\varphi}_0$  between the atoms in the central lattice site and in its  $j$ th nearest neighbor, we evaluate  $D_j$  defined as:

$$D_j \equiv |\langle e^{i(\hat{\varphi}_0 - \hat{\varphi}_j)} \rangle|. \quad (17)$$

Here  $\hat{a}_j = |\hat{a}_j| e^{i\hat{\varphi}_j}$  and  $D_j$  is calculated by normalizing  $\hat{a}_0^\dagger \hat{a}_j$  in each stochastic trajectory before the averaging. Typically  $D_j$  and  $C_j$  yield almost equal results and we usually only show  $C_j$ .

### C. Numerical approach

We study the nonequilibrium quantum dynamics of the bosonic atoms within the TWA. The BEC, which is initially confined in a harmonic trap, is split by a periodic multi-well optical lattice or a double-well potential. The atoms are initially assumed to be in thermal equilibrium and we first solve the ground state amplitude profile  $\psi_0(x)$  by evolving the GPE in imaginary time in the harmonic trap. We then diagonalize the Bogoliubov equations [Eq. (8)] in the subspace orthogonal to  $\psi_0(x)$  in order to obtain the quasiparticle eigenfunctions  $u_j(x)$ ,  $v_j(x)$  and the corresponding eigenenergies  $\epsilon_j$ .

Throughout the paper we use large atom numbers,  $N_0 = 2000$  atoms at the beginning of the ramp, so that

the occupation number of the central lattice sites is always high. For the typical nonlinearity  $N_0 g_{1D} = 100 \hbar \omega l$ , with  $l \equiv (\hbar/m\omega)^{1/2}$ , the corresponding initial Thomas-Fermi radius  $R/l = (3N_0 g_{1D}/2\hbar\omega l)^{1/3} \simeq 5.3$ . In 1D the strength of interactions is commonly expressed in terms of the ratio  $\gamma$  between the interaction energy and the kinetic energy needed to localize the atoms within the mean interatomic distance  $1/n_{1D}$ , where  $n_{1D}$  is the 1D atom density [50]. We obtain  $\gamma = m g_{1D}/(\hbar^2 n_{1D}) \lesssim 10^{-3}$  and the initial harmonically trapped BEC is well described by the GPE and the Bogoliubov theory.

The time evolution of the ensemble of Wigner distributed wavefunctions, determined by Eq. (5), is unraveled into stochastic trajectories, where the initial state of each realization for the classical stochastic field  $\psi_W$  is generated using the expansion (6) with the operators replaced by the complex, Gaussian-distributed [Eqs. (9) and (11)] random variables  $(\alpha_j, \alpha_j^*)$ . During the time evolution we continuously increase the strength of the periodic optical lattice potential or, in the case of the double-well, a repulsive Gaussian potential at the center of the trap. The integration of the time dynamics [Eq. (5)] is performed using the nonlinear split-step method [51] on a spatial grid of up to 4096 points and in several cases with the optical lattice potential the sufficient convergence is obtained after 600 realizations, whereas in a double-well potential typically around 800 realizations are required. The convergence is generally slower at higher temperatures. Finite temperature systems require more iterations and are therefore numerically more demanding. This is clear in the sampling of the Wigner distribution in Eq. (9) whose width increases with the initial temperature  $T_i$ , indicating higher excited level population and more noise in the initial state Wigner distribution. Unlike the 3D TWA [38], the 1D simulations do not similarly depend on the total number of quasiparticle modes and we found the calculated results to be unchanged when we varied the number of modes.

## III. SPLITTING A BEC BY AN OPTICAL POTENTIAL

### A. Double-well potential

Before turning to the dynamical studies of bosonic atoms fragmented by an optical lattice, it is useful first to introduce the TWA method in a much simpler double-well potential case. Since the projection method we found very useful in an optical lattice is much less accurate in a double-well potential for short nonadiabatic ramping-up times, we only present here some example cases and will publish a more detailed study elsewhere.

The splitting of a BEC by a double-well potential has attracted considerable theoretical interest in the past (see, e.g., Refs. [52, 53], and references therein). Also the finite-temperature dynamics of atomic BECs in a double-well potential has been investigated [54, 55]. Recent ex-

periments include, e.g., the use of a double-well BEC as a noise thermometer [56].

We use the similar set-up as in the early BEC experiment of Ref. [57], where a harmonically trapped BEC was split by a blue-detuned far-off resonant laser beam. We model the laser by a Gaussian potential in Eq. (2)

$$V_o(x, t) = A(t) \exp(-x^2/\sigma), \quad (18)$$

with  $\sigma = 0.5l^2$ . During the time evolution, we increase exponentially the laser potential to some final value  $A_f$  at time  $\tau$  according to  $A(t) = \exp(\kappa t) - 1$ . In Fig. 1 we show the dynamics of the phase coherence  $C_1$  between the two wells, as defined in Eq. (16). We vary the nonlinearity and the initial temperature. The ramping-up time of the Gaussian potential is  $\omega\tau = 5$ . As expected, both the increase in the nonlinearity and in the initial temperature result in a faster reduction of the relative phase coherence. However, the projection to the ground state in Eq. (13) in the double-well case resulted in notable atom number oscillations and the calculated phase coherence values should therefore be considered only as an order of magnitude estimates. We can compare the zero-temperature case of the collapse time of the relative phase coherence between the atoms in the two wells to the estimates obtained from the Bogoliubov theory for a ground state BEC [58]. If we generalize the results of Ref. [58] for the present situation and for arbitrary  $\Delta n$ , we obtain for the collapse time  $\tau_c$ :

$$\tau_c = 24^{1/3} \ln 2 \left( \frac{g_{1D}}{\hbar\omega l} \right)^{-2/3} \frac{n^{1/3}}{\omega\Delta n}. \quad (19)$$

After a time  $\tau_c$ , the value of the coherence function  $C_1$  is reduced to 0.5. The values of  $n$  and  $\Delta n$  in Eq. (19) could be obtained from the numerical results of the TWA simulations, e.g., by averaging  $\Delta n$  after the ramping process. If we assume the atom number fluctuations between the two wells to be Poissonian (or binomial), we obtain for the collapse times  $\omega\tau_c = 3.3, 2.5, 2.1$ , for the nonlinearities  $N_0 g_{1D}/(\hbar\omega l) = 100, 150, 200$ , respectively. The collapse time of the TWA simulations is estimated by determining the time when  $C_1 = 0.5$  and subtracting the ramping-up time  $\omega\tau = 5$  from this value. For the same nonlinearities we obtain  $\omega\tau_c > 5$ ,  $\omega\tau_c \simeq 5$ , and  $\omega\tau_c \simeq 4$ .

The collapse time for the phase coherence is quite sensitive to the atom number fluctuations and could be experimentally used to measure  $\Delta n$ . The collapse time in the TWA simulations indicates sub-Poisson atom number fluctuations. The simple collapse time estimate from Eq. (19), that does not take into account the effects of the dynamical splitting of the BEC, yields  $\Delta n \sim \Delta n_{\text{Poisson}}/2$ . The numerical values of  $\Delta n$  in the TWA simulations are not reliable because of the simple projection method used in the double-well problem.

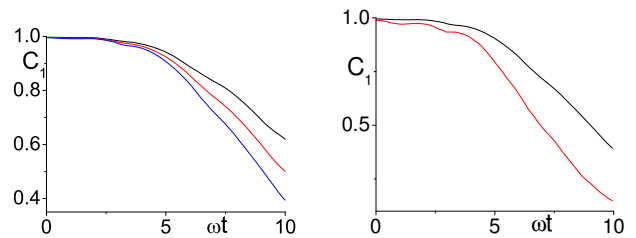


FIG. 1: The dynamics of the phase coherence during the splitting of a BEC by a Gaussian potential barrier. The phase coherence between the atoms in the two wells for different nonlinearities (on left)  $N_0 g_{1D}/(\hbar\omega l) = 100, 150, 200$  (the curves from top to bottom) at the initial temperature  $T_i = 0$ . The phase coherence at two different initial temperatures (on right)  $k_B T_i/\hbar\omega = 0$  and  $37.8$  (the lower curve) for  $N_0 g_{1D} = 200\hbar\omega l$ . In the both cases the final value of the Gaussian potential is  $A_f = 1000\hbar\omega$ , and its width  $\sigma = 0.5l^2$ . The ramping-up time is  $\omega\tau = 5$  and  $N_0 = 2000$ .

## B. Optical lattice with a small number of sites

The condensate fragmentation is generally much more difficult to analyze when the number of wells is increased from two [59]. The TWA, incorporating quantum and thermal fluctuations for the complete field operator, becomes a very useful tool in investigating the dynamics of the fragmentation process. Unlike in the double-well case, the projection method to the lowest mode in each site produces stable and more accurate results.

In this Section we demonstrate the loss of phase coherence between the atoms in different lattice sites, when the BEC is split by continuously turning up an optical lattice with a small number of sites. We evaluate the phase collapse both at  $T = 0$  and at finite temperature. In the following Section we turn to a more detailed study of the turning up process of the lattice potential when the number of lattice sites is larger.

We start with the system in thermal equilibrium in the harmonic trap and continuously turn up an optical lattice potential, so that  $V_o(x, t)$  in Eq. (2) is defined by

$$V_o(x, t) = s(t) E_r \sin^2(\pi x/d), \quad (20)$$

where the lattice photon recoil energy

$$E_r \equiv \frac{\hbar^2 \pi^2}{2md^2}, \quad (21)$$

and  $d = \lambda/2 \sin(\theta/2)$  denotes the lattice period, obtained by two laser beams intersecting at an angle  $\theta$ . The advantage of 1D lattices is that the lattice spacing can be easily modified by changing the angle between the lasers. In the simulations the height of the lattice potential  $s(t)$  is turned up exponentially during a time  $\tau$  to some final value  $s$  according to

$$s(t) = e^{\kappa t} - 1, \quad (22)$$

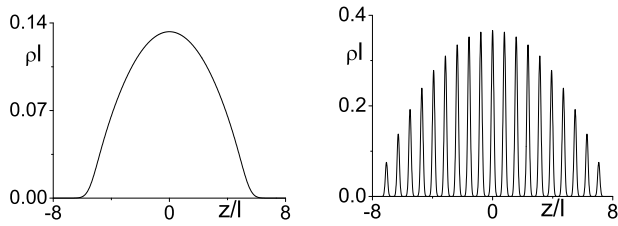


FIG. 2: The normalized ground state atom density in a harmonic trap without optical lattice (left) and with the lattice for  $s = 37.5$ . The lattice has clearly pushed the atoms towards the outer regions of the trap by increasing the radius of the atom vapor. The nonlinearity  $N_0 g_{1D} = 120\hbar\omega l$  and the wavenumber  $kl = 4$ .

for  $t \leq \tau$ . In this Section we use the lattice spacing  $d = \pi l/4$  and the nonlinearity  $N_0 g_{1D} = 120\hbar\omega l$ . For instance, the ground state calculated at the lattice height  $s = 37.5$  then occupies  $\sim 19$  sites; see Fig. 2. However, in a fast nonadiabatic turning up of the lattice, we study here, only about 13-15 wells are occupied after the ramping.

As the lattice is raised the tunneling amplitude of the atoms between the neighboring sites decreases exponentially and the system becomes more strongly interacting. The strong interactions in the lattice enhance quantum fluctuations, eventually destroying the long-range phase coherence of the atoms.

The relative phase between the atoms in different lattice sites during the turning up of the lattice potential generally indicates the flow of atoms towards the edges of the atom cloud, as the cloud radius increases due to the lattice. The dynamics of the phase on a single stochastic realization also undergoes stochastic fluctuations due to the vacuum noise. The deeper the lattice potential, the larger are the variations in the dynamical trajectories of the phase between individual stochastic realizations. These variations, once averaged over a large number of realizations, result in the loss of phase coherence.

In Fig. 3 we show the normalized phase coherence  $C_1$  for the atoms between the central well and its first neighbor, as defined in Eq. (16) at different initial temperatures  $T_i$ , for two different values of the ramping-up time. The phase collapse time exhibits exponential-like decrease as a function of  $T_i$  for  $\omega\tau = 1$ . We also show the phase coherence between the atoms in the central site and in its several nearest neighbors, describing the phase coherence along the lattice. The effect of the ramping-up time and the final lattice height on the phase coherence is shown in Fig. 4. It is interesting to note that in several cases the phase coherence rapidly decays during and immediately after the turning up of the lattice potential, but remains surprisingly steady at some finite value afterwards.

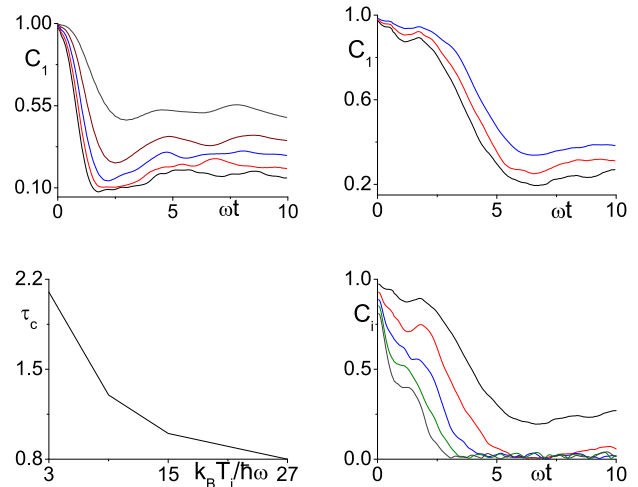


FIG. 3: The phase coherence at different temperatures and along the optical lattice. We evaluate  $C_1$  for the ramping-up times  $\omega\tau = 1$  (top left; curves from top correspond to the initial temperatures  $k_B T_i/\hbar\omega = 3, 9, 15, 21, 27$ ) and  $\omega\tau = 5$  (top right; curves from top correspond to  $k_B T_i/\hbar\omega = 15, 21, 27$ ). The notch after about one trap period in the coherence function is due to a resonance involving the first phonon modes  $u_1$  and  $v_1$  and is enhanced with the increasing temperature. The estimated phase collapse time  $\tau_c$  (bottom left) as a function of the initial temperature, obtained from the data in the top left diagram by choosing the time when  $C_1 = 0.65$ . The coherence between the atoms in the central site and in the first five nearest neighbors (bottom right; curves from top  $C_i$  with  $i$  from one to five) for  $k_B T_i = 27\hbar\omega$ . In all the plots  $N_0 g_{1D} = 120\hbar\omega l$ .

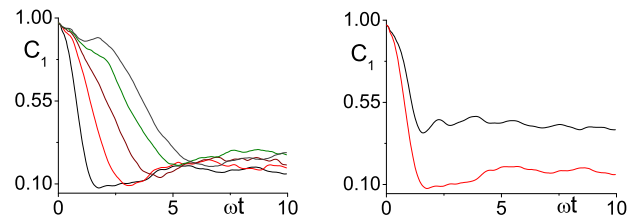


FIG. 4: The phase coherence for different ramping-up times and lattice height. The same system as in Fig. 3 at  $k_B T_i = 27\hbar\omega$  for different ramping-up times (on left; curves from left  $\omega\tau = 1, 2, 3, 4, 5$ ) and for the final lattice heights  $s = 37.5$  (lower curve) and  $s = 25$  (upper curve) for  $\omega\tau = 1$  (on right).

### C. Optical lattice with a larger number of sites

In this Section we present the main results of the paper by considering the splitting of a harmonically trapped BEC by a rapidly varying optical lattice potential. We choose the lattice spacing to be  $d = \pi l/8$  in Eq. (20). We then have about 30-35 lattice sites within the classical diameter  $2R$  of the BEC. A similar number of sites has also been realized in recent experiments in a cigar-shaped

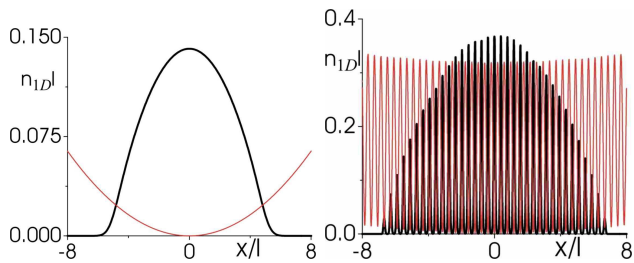


FIG. 5: The normalized ground state atom density (thick line) in a harmonic (left) and in a combined harmonic and optical lattice (right) with  $s = 20$ . For illustrative purposes we also show the potentials (thin line; in arbitrary units). Here  $N_0 g_{1D} = 100\hbar\omega l$  and  $kl = 8$ .

trap with  $d \simeq 2.7\mu\text{m}$  [4]. The ground state atom number  $N_0 = 2000$  before turning up the lattice results in the occupation number of about  $n_0 \simeq 90$ -100 atoms in the central site of the optical lattice. The normalized ground state atom density is shown in Fig. 5 with (for  $s = 20$ ) and without an optical lattice.

### 1. The effect of the final lattice height

In this Section we vary the final height of the optical lattice potential when a harmonically trapped BEC is fragmented by means of continuously turning up the lattice. We evaluate the dynamics of the phase fluctuations between the atoms in different lattice sites and the atom number fluctuations in individual sites. The system is closely related to the recent experiment by Orzel *et al.* [6] where the atom number squeezing in strong optical lattices with large filling factors was observed. However, the notable difference between our model and the experimental set-up is that in Ref. [6] the 1D optical lattice exhibited a very weak radial confinement and did not produce a tightly-elongated 1D gas with negligible radial excitations.

In Fig. 6 we show the phase coherence between the atoms in the central well and in its nearest neighbor  $C_1$  [Eq. (16)] and the number fluctuations  $\Delta n_0$  [Eq. (15)] in the central well for different final heights of the periodic potential at  $T = 0$ . The ramping-up time is fixed to  $\omega\tau = 6$  for  $s = 30, 40$  and to  $\omega\tau = 10$  for the shallower lattices. For shallow lattices the phase coherence remains high and steady, but for larger  $s$  it is reduced and becomes strongly oscillatory. The enhancement of phase fluctuations in deeper lattices is associated with progressively increasing atom number squeezing. The number squeezing can be accurately fitted according to

$$\frac{(\Delta n_0)^2}{n_0} \simeq 0.03 + 0.5e^{-s/8}. \quad (23)$$

Due to the large occupation numbers,  $\Delta n_0$  are strongly sub-Poissonian, approaching the asymptotic value  $(\Delta n_0)^2/n_0 \simeq 0.03 \ll 1$  for large  $s$ . The numer-

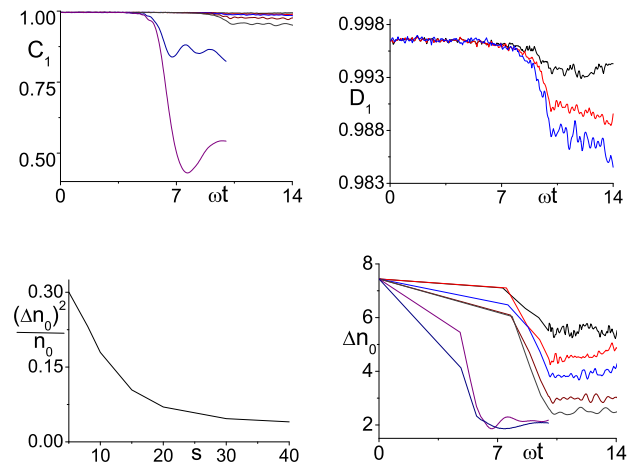


FIG. 6: The phase coherence between the central well and its nearest neighbor  $C_1$  as a function of time (top left) at  $T = 0$  for different final heights of the optical lattice (curves from top represent  $s = 5, 8, 10, 15, 20, 30, 40$  with the atom number in the central well  $n_0 \simeq 90$ -100). The ramping-up time  $\omega\tau = 10$ , except for  $s = 30, 40$ ,  $\omega\tau = 6$ . Top right:  $D_1$  for  $s = 5, 8, 10$  (curves top to bottom). The number fluctuations  $\Delta n_0$  for the central well (bottom right) for the same runs. Here  $g_{1D} = 0.05\hbar\omega l$  and  $N_0 = 2000$ . The number squeezing (bottom left) as a function of the final lattice height can be accurately fitted according to Eq. (23).

ics proved more demanding when the final height of the optical potential reached  $30$ - $40E_r$ .

Although the discrete tight-binding Hamiltonian Eq. (A1) is only valid for weakly excited and very deep lattices, it is interesting to compare the TWA to the Bogoliubov approximation of the BHH (A1), introduced in Appendix A. The discrete Bogoliubov result for the ground state in a uniform lattice [Eq. (A16)] predicts the phase fluctuations  $\Delta\varphi_{0,1}$  to be weak when the hopping amplitude  $J$  times the lattice site occupation number  $n$  is much larger than the on-site interaction  $U$ . From the numerical results for  $D_1$  [Eq. (17)] in Fig. 6 we can deduce  $(\Delta\varphi_{0,1})^2$  and for shallow lattices we find it to be roughly by the factor of two smaller than the uniform ground state result Eq. (A16). The small phase fluctuations of the TWA results may be better understood when we compare them to the phase fluctuations obtained by solving the discrete Bogoliubov theory in a combined harmonic trap and an optical lattice; Fig. 14. Including the harmonic trap can significantly reduce the phase fluctuations close to the trap center and enhance them close to the edge of the atom cloud.

The Bogoliubov result of the discrete tight-binding Hamiltonian Eq. (A1) for the ground state atom number fluctuations [Eq. (A15)] indicates that  $\Delta n_i$  becomes strongly sub-Poissonian ( $\Delta n_i^2 \ll n_i$ , when  $n_i U \gg J$ ). The numerical TWA results for the atom number fluctuations in shallow lattices in Fig. 6 are clearly higher than the homogeneous ground state result in Eq. (A15). More-

over, in deep lattices (see the discussion in Appendix A), the system in the ground state may undergo a quantum phase transition from the superfluid to the Mott insulator state. Here  $n_i J \sim U$  at  $s \simeq 38$ . However, in the simulations we find  $\Delta n_0 \gtrsim 1$  for all  $s$ . The saturation of the atom number squeezing in Eq. (23) and clearly higher values of  $\Delta n_0$  than predicted for the ground state indicate that the atoms are not loaded adiabatically into the optical lattice. The saturation can be understood if we take into account the effects of the finite ramping-up time of the lattice.

In order to preserve the adiabaticity during the turning-up of the lattice potential and for the system to remain in its ground state, we require that the rate of change of any parameter in the Hamiltonian to be slower than any characteristic time scale of the system. In optical lattices when the lattice height is increased, the most rapidly changing parameter typically is the tunneling amplitude for the atoms between neighboring sites. On the other hand, at low lattice heights it is more difficult to avoid exciting higher vibrational levels within one potential well, resulting in excitations in the higher energy bands.

The phonon mode energies  $\omega_j$  in the lowest energy band decrease with increasing lattice strength [see the homogeneous Bogoliubov result for the tight-binding Hamiltonian in Eq. (A12)] [60, 61] and, as the lattice becomes deeper, it is progressively more difficult to maintain the adiabaticity with respect to these excitations. In deep lattices for the loading to remain adiabatic it is therefore required that

$$\zeta(t) \equiv \left| \frac{1}{J(t)} \frac{\partial J(t)}{\partial t} \right| \ll \omega_j(t), \quad (24)$$

for all the phonon mode energies  $\omega_j$  during the turning up of the lattice.

In Fig. 6 we find the number squeezing to saturate around  $s=20-30$ , indicating the point where an increasing number of phonon modes is excited and the phonon mode frequencies no longer satisfy the condition Eq. (24). Consequently, the turning up of the lattice potential is strongly nonadiabatic. Due to the nonadiabaticity, the  $s \geq 15$  cases exhibit significant excess number fluctuations as compared to the ground state. After a short time period over which  $C_1$  remains constant, the large  $\Delta n_i$  evolve into large phase fluctuations and  $C_1$  becomes oscillatory and collapses.

As argued in Ref. [60], if the adiabaticity of a phonon mode breaks down, the number fluctuations of the mode freeze to the value that prevails at the time this occurs, i.e., when  $\omega_j \sim \zeta(t)$ . If we naively apply this argument to the Bogoliubov result in Eq. (A15) for the case where the adiabaticity condition Eq. (24) breaks down for several modes with  $\omega_j \lesssim \zeta(t)$ , we obtain

$$(\Delta n)^2 \simeq \sum_j \frac{\hbar \zeta_j(t_j)}{2UN_p}, \quad (25)$$

where  $\zeta_j(t_j)$  denotes the value of  $\zeta(t)$  when we have  $\omega_j \sim \zeta(t)$  for the first time during the turning up of the lattice for the  $j$ th phonon mode at time  $t_j$ . Since for all  $j$ ,  $\zeta_j(t_j)$  is in the studied case roughly of the order of  $\omega$ , we have the asymptotic value for  $s \rightarrow \infty$ ,

$$(\Delta n_i)^2 \sim \frac{\hbar \omega}{U}, \quad (26)$$

qualitatively similar to the results in Fig. 6.

We may also estimate in this case the time required to turn up the optical lattice adiabatically from  $s = 10$  to  $s = 35$ . If, for simplicity, we assume that the optical lattice was ramped up in such a way that  $J(t) \simeq J_0 e^{-\kappa t}$ , we obtain in Eq. (24) a constant  $\xi = \kappa$ . In order to have an adiabatic loading of the atoms into the lattice, we therefore require that  $\kappa \ll \omega_j$  for all the modes  $j$ . If we assume that the homogeneous Bogoliubov result Eq. (A14) for the lowest phonon mode energy  $\omega_{q,\min}$  still provides at least the correct order of magnitude estimate at  $s = 35$  with the large filling factor considered here, the adiabaticity condition is roughly satisfied if  $\kappa \ll 0.1/\omega$ . The corresponding time required to have a slow enough ramping from  $s = 10$  to  $s = 35$  is then  $\Delta t \gg 40/\omega \simeq 0.6\text{s}$ , where we have used the value of the trap frequency  $\omega = 2\pi \times 10\text{Hz}$  (with the present set of parameters this corresponds to the lattice spacing  $d \simeq 1.3\mu\text{m}$  for  $^{87}\text{Rb}$ ). However, such a slow turning up process of possibly tens of seconds in order to reach the Mott ground state is extremely difficult to achieve experimentally, since the ground state lifetime is limited by the losses due to the three-body collisions and the spontaneous emission of photons.

A similar argument also applies to the atom number squeezing experiment in Ref. [6]. In Ref. [6] a BEC was initially confined in a harmonic trap. The atom cloud was then split by continuously turning up an optical lattice and the atoms were interfered at different final heights of the lattice potential. The atom number squeezing in individual lattice sites was calculated from the phase fluctuations by measuring the loss of visibility in the interference fringes. The lattice had about 12 sites with  $\sim 1000$  atoms in the central well. The lattice depths of up to  $s = 50$  were reached, corresponding to  $n_i U/J \sim 10^5$ . Here  $n_i U$  was estimated from the size of the atom cloud and it varied considerably during the ramping, since the lattice light field also changed the transverse confinement depending on the lattice height. If we use the same simplified analysis as before to estimate the time required to turn up the lattice adiabatically from  $s = 10$  to  $s = 50$ , we obtain  $\Delta t \gg 50\text{ms}$ . Consequently, it is not surprising that the ramping-up time 200ms used in the experiments was not sufficiently slow to reach the ground state of the atoms. The adiabaticity condition  $\Delta t \gg 50\text{ms}$  is not as severe as in our simulation example, but in the system of Ref. [6] even the lattice height  $s = 50$  is still far below the Mott transition point.

As we already argued in Ref. [30], the requirement of a very slow ramping-up time generally makes it difficult

to reach the Mott insulator ground state experimentally when there are many atoms per lattice site for a large number of sites. This indicates that producing technologically interesting strong atom number squeezing with large occupation numbers has serious limitations. In the lattices with small filling factors, that have been so far used in the Mott insulator state experiments, the above argument is no longer valid due to rapidly emerging energy gap and much larger quantum fluctuations even in a shallow lattice.

We have shown that for large filling factors the squeezing of atom number fluctuations within individual lattice sites, resulting from the turning up of the lattice potential, saturates for deep lattices. The saturation of the number squeezing for strong lattices was experimentally observed in Ref. [6]. As we already pointed out, such a system is not tightly elongated, but we can still make qualitative comparisons to the experimental data. Although the saturation was assumed in Ref. [6] to be an artifact of the analysis method of the interference measurement, we also numerically find similar saturation effect in a qualitative agreement with the experiment, without including the effects of the interference experiment. As we argued here, such saturation may result as a consequence of the nonadiabaticity of the loading process.

If the loading is sufficiently rapid or the final lattice sufficiently high, so that the adiabaticity breaks down for a large number of modes, the optimal number squeezing is proportional to the ramping speed itself and the nonlinearity. Both in Fig. 6 and in Ref. [6] the squeezing saturates at about 15dB when  $n_i U/J \sim 10^4$ . The ramping-up time  $\tau \simeq 4000\hbar/E_r$  in Ref. [6] is one order of magnitude longer than in Fig. 6, but this is compensated by the weaker hopping amplitude  $J$ , so that the saturation roughly occurs at the same value of  $\omega_n \tau$ .

Due to the nonadiabaticity of the loading of atoms into the lattice, the system in Ref. [6] may not have been in its ground state during the turning up of the lattice potential. Similarly to our numerical example, the nonadiabaticity in the experiment can induce larger phase fluctuations than those in the Heisenberg minimum uncertainty state for the atom number and phase. Additionally, an inhomogeneous phase profile can reduce the visibility of interference fringes similarly to phase fluctuations. Consequently, not all the experimentally detected phase noise in the loss of interference fringes may directly correspond to the atom number squeezing. Although the increased phase noise in the experiment therefore did not provide an entirely conclusive measure of the atom number fluctuations, our numerical simulations, nevertheless, seem to indicate that a considerable number squeezing may have been present also in Ref. [6].

The effect of increased phase fluctuations due to a rapid turning up of the lattice may even be more pronounced in the absence of strong radial confinement, as in Ref. [6], as a result of the nonlinear coupling between the radial and the axial modes. The numerical solution of GPE in 1D, in Ref. [31], and in 3D, in Ref. [32], was com-

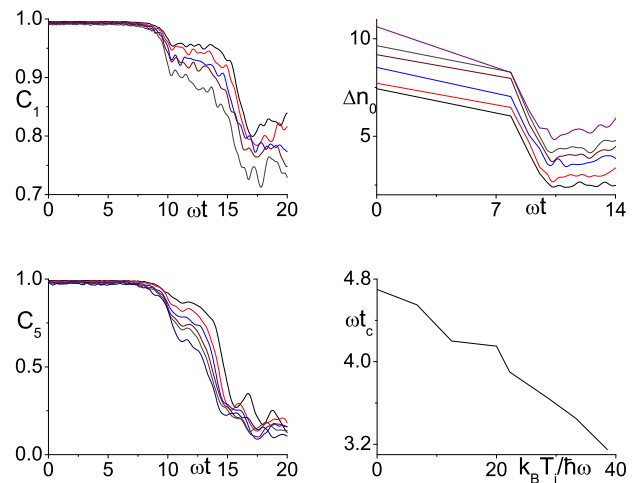


FIG. 7: The phase coherences  $C_1$  (top left),  $C_5$  (bottom left) and the number fluctuations  $\Delta n_0$  (top right) for initial temperatures (curves from top)  $k_B T_i / \hbar\omega = 0, 12.5, 22.2, 33.3, 38.5$  ( $C_5$  also with 28.5). The phase collapse time  $t_c$  (bottom right) is evaluated at  $C_5 = 0.5$ , subtracting the ramping-up time. Here  $N_0 g_{1D} = 100\hbar\omega l$ ,  $N_0 = 2000$ ,  $\omega\tau = 10$ , and  $s = 20$ .

pared to the experimentally observed phase noise using the parameters of Ref. [6]. Although this model cannot incorporate any quantum effects, the numerics showed signs of a reduced interference visibility due to inhomogeneous phase profile [62].

## 2. The effect of initial temperature and nonlinearity

Finite initial temperature increases the initial noise in the Wigner distribution [Eq. (9)] of the TWA as a consequence of the finite temperature noncondensate fraction in the excited levels. This is expected to affect the coherence between the different sites (as we saw in Section III B) and the fluctuations in the atom number  $\Delta n_0$ . In Fig. 7 we show  $\Delta n_0$  and the phase coherence  $C_1$  for different initial temperatures  $T_i$  for final lattice height  $s(\tau) = 20$ . Here  $(\Delta n_0)^2$  increases exponentially as a function of  $T_i$ . The phase coherence  $C_5$  between the central well and its fifth neighbor decays significantly faster than  $C_1$ . The dependence of the phase collapse time  $\tau_c$  on the initial temperature  $T_i$  is approximately linear (compare to Fig. 3). At  $s = 20$  the effects of the harmonic trap are already significant in  $C_5$ , since the potential energy difference due to the harmonic trap between the central lattice site and its fifth nearest neighbor exceeds the tunneling energy  $V_h(j=5) - V_h(j=0) \simeq 2\hbar\omega \gtrsim n_0 J$ .

In order to estimate the effect of the nonlinearity we varied  $N_0 g_{1D} / (\hbar\omega l)$  from 100 to 200 for the case of the final lattice height  $s = 20$ , the ramping-up time  $\omega\tau = 10$ , and the initial temperature  $T_i = 0$ . In Fig. 8 we show the results for the phase coherence  $C_5$  and the atom number fluctuations  $\Delta n_0$  in the central well. The depen-

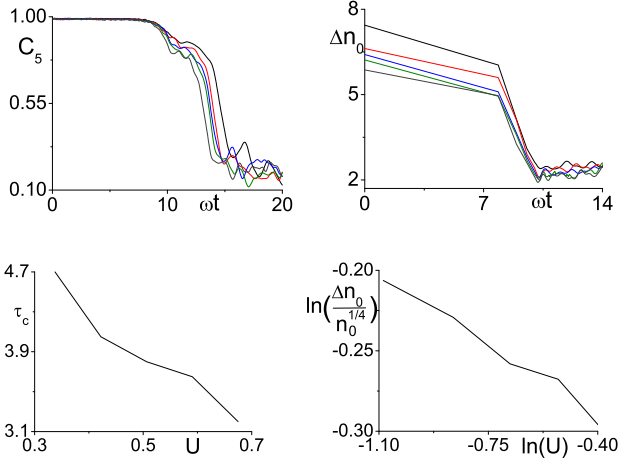


FIG. 8: The coherence function  $C_5$  (top left) and the number fluctuations in the central well (top right). The curves from top represent  $N_0 g_{1D}/(\hbar\omega l) = 100, 125, 150, 175, 200$ . The collapse time (evaluated when  $C_5 = 0.5$  and subtracting the ramping-up time) (bottom left) and  $\Delta n_0/n_0^{1/4}$  (bottom right) as a function of the on-site interaction  $U$  (in the units of  $\hbar\omega$ ) at  $T_i = 0$ . Here  $N_0 = 2000$ ,  $s = 20$ , and  $\omega\tau = 10$ .

dence of the phase collapse time on the nonlinearity is obtained by choosing the time when  $C_5 = 0.5$ . We compare the numerical TWA results for  $\Delta n_0$  to the analytic tight-binding result in the ground state of the uniform lattice (A17) by fitting the TWA results according to  $(\Delta n_0)/\sqrt{n_0} \propto U^c$ . Here the exponent  $c$  of the on-site nonlinearity is the fitting parameter. The TWA simulations yield  $c \simeq -0.3$ , as compared to the ground state result  $c = -0.5$  of Eq. (A17). In Fig. 8, the  $(\Delta n_0)/\sqrt{n_0}$  plot was obtained by averaging over the time interval  $4/\omega$  after the lattice was turned up.

### 3. Validity of the classical GP theory

The classical mean-field theories, in particular the GPE, have been very successful in describing the full multi-mode dynamics of weakly-interacting, harmonically trapped atomic BECs. However, the GPE has severe limitations in optical lattices where the interactions are enhanced, since the classical GPE disregards thermal and quantum fluctuations, decoherence, and the information about quantum statistics. It is especially interesting to study the limits of validity of the GPE in shallow optical lattices. In Ref. [43] it was shown that the experimentally observed damping of the dipolar motion of atoms in a very shallow lattice with  $s = 0.25$  [11] resulted from the large ratio  $g_{1D}/N$ . If the atom number in the simulations was increased, or  $g_{1D}/N$  decreased, while at the same time keeping the chemical potential  $\propto N g_{1D}$  fixed, the damping rate was reduced exponentially and the results approached the classical GPE limit. Here we study the turning up of the lattice for much larger filling

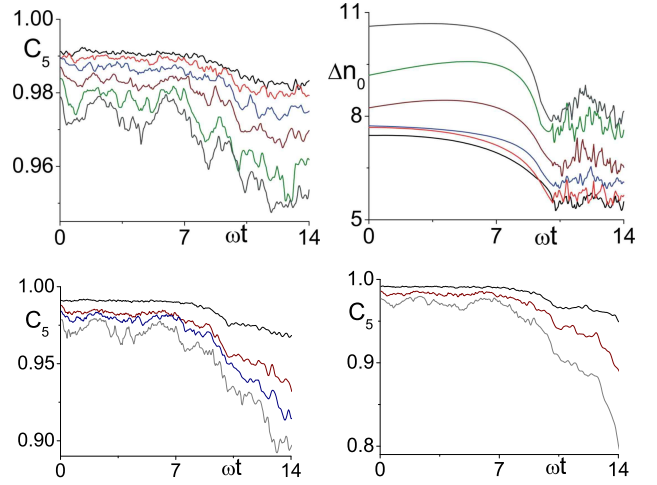


FIG. 9: The coherence  $C_5$  between the central well and the fifth neighbor (top left) and the atom number fluctuations in the central well  $\Delta n_0$  (top right) for the case of the final lattice height  $s = 5$ . The curves from top represent the initial temperatures  $k_B T_i/\hbar\omega = 0, 6.67, 12.5, 22.2, 33.3, 38.5$ . The phase coherence  $C_5$  for  $s = 8$  (bottom left) and for  $s = 10$  (bottom right). The curves from top represent the initial temperatures  $k_B T_i/\hbar\omega = 0, 22.2, 28.6, 38.5$  and  $0, 22.2, 38.5$ , respectively. The nonlinearity  $N_0 g_{1D} = 100\hbar\omega l$ ,  $N_0 = 2000$ , and the ramping-up time  $\omega\tau = 10$ .

factors and, hence, smaller  $g_{1D}/N$ .

In Fig. 9 we show the coherence between the central well and its fifth neighbor for different final lattice heights and different temperatures and the atom number fluctuations in the central well for  $s = 5$ . The number of atoms in the central site  $n_0 \simeq 90-100$ . For the case of  $s = 5$  the phase coherence remains high at low initial temperatures. The number fluctuations at  $T_i = 0$  are weakly sub-Poissonian  $\Delta n_0 \simeq 5.5 < 10$  and are increased due to the initial finite temperature. However, for  $s = 8$  and  $s = 10$ , the TWA results are notably different from the classical GPE dynamics, even at zero temperature. For  $s = 8$  and  $s = 10$  the loss of coherence at  $T_i = 0$  due to vacuum fluctuations is already comparable to the loss of coherence at  $s = 5$  due to thermal fluctuations at  $k_B T_i = 38.5\hbar\omega$ . (When the initial thermal population is close to ten percent.) For  $s = 10$ , the atom number fluctuations are also more sub-Poissonian  $\Delta n_0 \simeq 3.9 < 10$  at  $T_i = 0$ ; see Fig. 6.

### 4. Change of temperature during the splitting

The optical potential also affects the temperature of the atom vapor. If the lattice potential is turned up adiabatically, the population of each mode remains constant and temperature  $T$  can change dramatically, as the contribution of each mode to  $T$  changes by the ratio of the final and initial mode energies  $\omega_j^{(f)}/\omega_j^{(i)}$ . An adia-

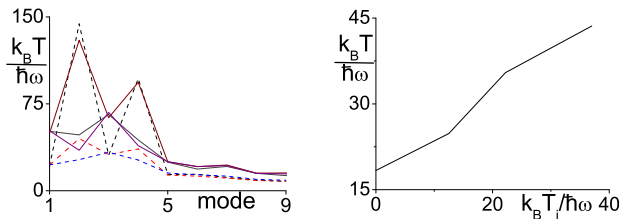


FIG. 10: The contribution of the lowest modes to temperature (left) for  $k_B T_i / \hbar\omega = 12.5$  (dashed line) and 37 (solid line). Curves from top to bottom represent  $\omega\tau = 10, 20, 30$  in both cases. The average temperature of the first five modes after the ramping  $\omega\tau = 30$  (right) for an initial temperature  $k_B T_i = 0, 12.5, 22.2, 37$ . Here  $g_{1D} = 0.015\hbar\omega l$ ,  $N_0 = 2000$ , and  $s = 5$ .

batic increase in the lattice strength may both increase or lower  $T$ , depending on whether the excited band is occupied [63] and in the experiments the condensation temperature has been found to be sensitive to the lattice height [64]. In Fig. 10 we estimated the ‘temperature’ of several lowest phonon modes in the TWA simulations by evaluating the corresponding occupation numbers  $\bar{n}_k$ . This was obtained by calculating the projection of  $\psi_W$  to the Bogoliubov modes of the BHH using Eq. (A6), as explained in Appendix A. The averages are taken over a time period before any significant rethermalization occurs after the ramping [65]. The modes 2 and 4 are highly excited for the case of short  $\tau$ , due to the nonadiabatic loading. The excitations are damped out at higher initial temperatures  $T_i$  and for the case of the slowest ramping  $\omega\tau = 30$ , representing the situation where  $\omega_2\tau \gg 1$  and  $\omega_4\tau \gg 1$ . It is interesting to note that the excitations of the fourth mode are only damped out when the rate of change in the tunneling amplitude  $\zeta$  is much smaller than the corresponding mode energy, or when  $\omega_4 \simeq 26\zeta(\tau)$ . This is more restrictive condition than the one found in Ref. [60]. For very fast ramping  $\omega\tau \lesssim 3$ , the variation of  $T_i$  is already completely dominated by the excitations due to the rapid turning up of the lattice.

### 5. Turning up the nonlinearity

The numerical solutions for the initial equilibrium state in the TWA simulations may in some cases, especially in higher dimensions, be difficult to obtain. In Ref. [42] the ideal, noninteracting condensate was used as an initial state for the TWA simulations, but the interaction constant was first continuously ramped from zero up to some final value, before the actual atom dynamics was studied. By means of turning the nonlinearity up slowly enough, the goal was to produce the initial state of an interacting system. If the ramping is slow enough, the dynamics is then expected to resemble to that of the interacting system. Here we study the atom dynamics by first linearly turning up the interaction constant from

$g_{1D}^{\text{initial}} = 0$  to a final value  $g_{1D}^{\text{final}}$  during the time  $\tau_g$ , before starting to ramp up the optical potential. Experimentally, such a technique could possibly be employed by means of using Feshbach resonances to tune the value of the scattering length  $a$ .

The field operator for the initial state of the noninteracting system is that of the ideal harmonic oscillators in thermal equilibrium:

$$\hat{\psi}(x, t = 0) = \frac{\hat{\alpha}_0}{\pi^{1/4} l^{1/2}} \exp\left(-\frac{x^2}{2l^2}\right) + \sum_{j>0} \hat{\alpha}_j R_j H_j(x/l) \exp\left(-\frac{x^2}{2l^2}\right), \quad (27)$$

where we have explicitly separated the BEC mode,  $H_j$  is the  $j$ th Hermite polynomial, and  $R_j \equiv (\sqrt{\pi} 2^j j!)^{-1/2}$ . The sampling of the Wigner distribution for  $\alpha_j$  and  $\alpha_0$  to generate  $\psi_W(x, t = 0)$  is then performed exactly as in the interacting case.

In Fig. 11 we show the TWA simulation results for the initially noninteracting system for which we first slowly turn up the interactions to the value  $g_{1D} = 0.05\hbar\omega l$ , before ramping up the optical lattice potential. We also show the results for the initially interacting system for which the initial state is obtained by solving the Bogoliubov equations with  $g_{1D} = 0.05\hbar\omega l$ . The initial temperature of the noninteracting case is set to be equal to the temperature of the interacting system we want to compare. Therefore the condensate and the noncondensate populations in the initial state of the TWA simulations are slightly different in the interacting and noninteracting cases.

In the example case the two approaches yield surprisingly similar results at low  $T_i$ . At higher  $T_i$  the atom number fluctuations in the case of the ideal gas initial state are smaller. This is most likely due to the lack of any notable rethermalization in the 1D TWA simulations [65], so the turning up of the nonlinearity fails to produce the thermal equilibrium state.

### 6. Sampling of the noise for the initial ground state mode

In the TWA simulations the quantum fluctuations of the initial BEC mode are included by assuming the BEC to be in a coherent state, so that the initial state is sampled according to the corresponding Wigner distribution in Eq. (11). Although the condensate mode is expected to exhibit sub-Poisson atom number fluctuations, the advantage of the coherent state representation is that the Wigner distribution is positive. For instance, the Wigner distribution of a number state with  $n$  atoms is nonpositive:  $W(\alpha, \alpha^*) = 2(-1)^n \exp(-2|\alpha|^2) L_n(4|\alpha|^2) / \pi$  [48], where  $L_n$  denotes the Laguerre polynomial, and cannot be represented in the TWA simulations without doubling the dimension of the phase space [66] analogously to the positive P representation [47]. However, as we already

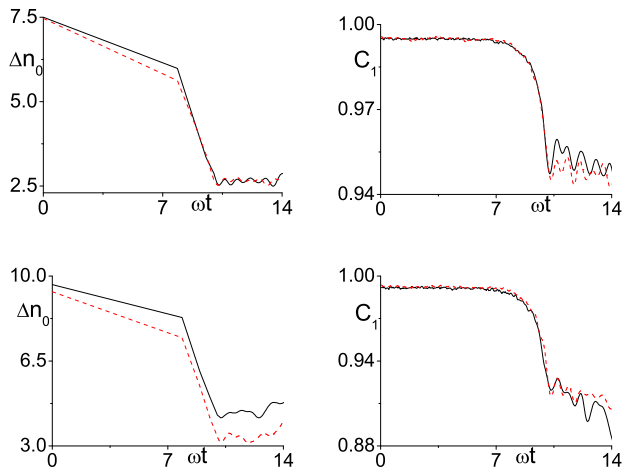


FIG. 11: The phase coherence and the number fluctuations for an initially noninteracting system ( $g_{1D}^{\text{initial}} = 0$ ) with the interactions linearly turned up to the value  $g_{1D}^{\text{final}} = g_{1D} = 0.05\hbar\omega l$  (dashed red line) and in an initially interacting system (solid black line), obtained by solving the Bogoliubov equations for  $g_{1D} = 0.05\hbar\omega l$  with  $N_0 = 2000$ ,  $s = 20$ , and  $\omega\tau = 10$ . The initial temperature is  $k_B T_i / \hbar\omega = 6.67$  (on top) and  $33.33$  (at bottom) and the ramping-up time of the nonlinearity  $\omega\tau_g = 15$ . The results for the evolution of the ideal gas describe its dynamics after the end of the ramping of the nonlinearity.

noted earlier, the particular representation is not so crucial, since the main contribution to the matter wave coherence is due to the thermal and quantum fluctuations of low-energy phonons and the quantum fluctuations of the initial state of the BEC mode are not very important. In Fig. 12 we show the TWA results for the typical physical parameters of our system both when the BEC mode is sampled according to Eq. (11) (with Poisson atom number fluctuations) and when we entirely ignore the quantum fluctuations of the BEC mode and treat it classically having a fixed number of atoms. A classical treatment of the ground state does not affect the prediction for the phase coherence along the lattice, but produces slightly smaller atom number fluctuations in the lattice sites.

### 7. Importance of the symmetric ordering

The TWA simulations return quantum expectation values for the operators that are symmetrically ordered. This generally creates significant complications in interpreting the simulation results in terms of normally ordered expectation values, as we already emphasized in Section II B. However, as we here demonstrate, the correct transformation between the different operator orderings is very crucial in obtaining the correct physical results.

Since the P-representation of the density matrix re-

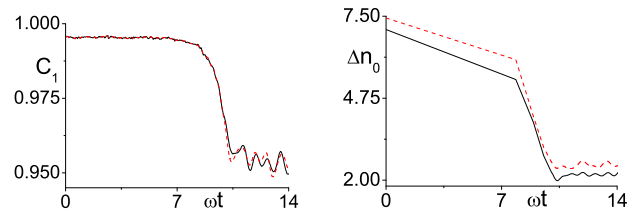


FIG. 12: The phase coherence  $C_1$  and the atom number fluctuations  $\Delta n_0$  for cases where the initial ground state was simulated classically with a fixed number of atoms (solid black line) and where the initial ground state included quantum fluctuations while assuming a coherent state (dashed red line). Here  $T_i = 0$ ,  $N_0 g_{1D} = 100\hbar\omega l$ ,  $N_0 = 2000$ ,  $s = 20$ , and  $\omega\tau = 10$ .

turns the expectation values of normally ordered operators, e.g.,  $\langle \alpha_j^* \alpha_j \rangle_P = \langle \hat{\alpha}_j^\dagger \hat{\alpha}_j \rangle$ , we may also call the stochastic dynamics that assumes the operator expectation values to be normally ordered as the “truncated P approximation” (TPA) [38]. The P-representation is singular at  $T = 0$ , but is often used to study finite temperature systems. A review of its mathematical properties may be found in Refs. [47, 48].

We illustrate with a numerical example the importance of the particular stochastic representation of the density matrix. We integrate both TWA and TPA according to Eq. (5) for the same system at finite initial temperature  $T_i$  by means sampling the Wigner and the  $P$  distributions. The results shown in Fig. 13 for the phase coherence  $C_1$  and the atom number fluctuations  $\Delta n_0$  are then useful in understanding the importance of the operator ordering. The P-distribution does not introduce the correct noise in the initial state and therefore it fails to produce the right phase coherence properties and underestimates the atom number fluctuations. At high temperature, the TPA is closer to the TWA because thermal noise starts dominating vacuum fluctuations.

## IV. CONCLUDING REMARKS

We studied the loading of a harmonically trapped BEC into an optical lattice. As the lattice height is increased, quantum fluctuations become more important and the classical GP description breaks down. We found that the TWA provides a powerful tool to study nonequilibrium dynamics of bosonic atoms in an optical lattice. We showed that, especially at low temperatures, the correct quantum statistics of phonon modes and the accurate treatment of the operator orderings in the Wigner representation are very important.

The TWA incorporates the full multi-band description of the lattice dynamics and becomes more accurate when the occupation number of the sites is large and quantum fluctuations are not too dominating. In the TWA simulations of the turning up of the lattice potential we

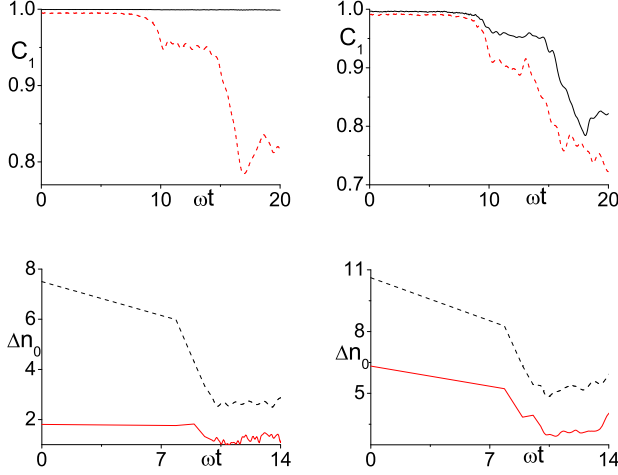


FIG. 13: The phase coherence and the atom number fluctuations, obtained by taking into account the symmetric operator ordering in the TWA (dashed line) and by assuming the stochastic representation to be normally ordered (solid line) for an initial temperature of the system  $k_B T_i / \hbar \omega = 6.67$  (left) and 38.46 (right). The same system as in Fig. 12.

found the atom number squeezing to saturate for deep lattices, which can be explained by the finite turning-up time. It is numerically more demanding to study significantly longer ramping-up times that would result in considerably more reduced atom number fluctuations. It is also expected that the TWA would eventually break down over longer time scales very close to the MI state that could be interesting to investigate. In our theoretical study of dissipative dipole oscillations of bosonic atoms [43], we successfully modeled the system with the TWA for the case of considerably stronger quantum fluctuations than in the present work, in a good agreement with the experimental results [11]. This seems to suggest that also notably stronger atom number squeezing could be studied within the TWA than the one reported in this paper by considering very long ramping-up times. As our analysis shows, however, that, in the case of lattices with large filling factors, very long ramping-up times, that are required to reach the MI ground state, can be extremely challenging in actual experiments.

The TWA simulations could also be extended to 2D or 3D lattices. In 2D and 3D the implementation of the TWA may require a special care, but, at least in the uniform space, it has been successful in modeling thermal fluctuations [38]. In higher dimensions also more complex initial states could be considered, such as topological defects and textures that may be prepared by phase imprinting [67].

## APPENDIX A: BOGOLIUBOV THEORY IN A DISCRETE TIGHT-BINDING APPROXIMATION

It is useful to compare the TWA simulation results to the ground state fluctuations of the atoms, obtained from the Bogoliubov theory. In a deep optical lattice, with very large  $s$ , and close to the ground state only one mode per lattice site is important and the system can be approximated by the discrete Bose-Hubbard Hamiltonian (BHH), where we expand the field operator on the basis of the Wannier functions and keep only the lowest vibrational states in each lattice site,  $\hat{\psi}(x) = \sum_i \hat{b}_i \eta_i(x)$ :

$$H = \sum_i [\nu_i \hat{b}_i^\dagger \hat{b}_i - J(\hat{b}_i^\dagger \hat{b}_{i+1} + \text{H.c.}) + \frac{U}{2} (\hat{b}_i^\dagger)^2 \hat{b}_i^2], \quad (\text{A1})$$

where the summation is over the lattice sites,  $J \simeq -\int dx \eta_i^*(x) \mathcal{L} \eta_{i+1}(x)$  is the hopping amplitude between the nearest-neighbor sites,  $U \simeq g_{1D} \int dx |\eta_j(x)|^4$  is the on-site interaction constant, and  $\nu_j \equiv j^2 d^2 m \omega^2 / 2$  represents the harmonic trapping potential, with  $j = 0$  site at the trap center. We may approximate the Wannier functions  $\eta_i$  by the ground state harmonic oscillator wave function with the frequency

$$\omega_s = \frac{2s^{1/2} E_r}{\hbar}, \quad (\text{A2})$$

which is obtained by expanding the optical potential at the lattice site minimum [68]. Analytic approximations for  $U$  and  $J$  may be derived using the Gaussian approximations to the Wannier wave functions or the Matthieu functions of the energy band. When we compare the TWA results to the BHH, we frequently extract the expectation values involving  $\hat{b}$  using Eq. (13) with  $\hat{b} \sim \hat{a}$ . We tested that using different projections does not affect the results. For  $n_i J \gtrsim U$ , with  $n_i \equiv \langle \hat{b}_i^\dagger \hat{b}_i \rangle$ , the system is in the superfluid regime with the long-range phase coherence and is expected to undergo the MI transition at  $2.2n_i J \simeq U$  [69, 70], resulting in a highly number squeezed ground state.

In the Bogoliubov approach to the BHH we introduce the discrete position coordinate is  $x = jd$ , where  $j$  is the integer labeling the lattice sites. We decompose the ground state and the excited state fractions into mutually orthogonal subspaces and study the linearized fluctuations around  $c_j \equiv \langle \hat{b}_j \rangle$ :

$$\begin{aligned} \hat{b}_j &= c_j + \delta \hat{b}_j \\ &= c_j + \sum_n [f_n(jd) \hat{\chi}_n - h_n^*(jd) \hat{\chi}_n^\dagger], \end{aligned} \quad (\text{A3})$$

where  $\chi_n$  are the quasiparticle operators and  $[f_n(jd), h_n(jd)]$  are the Bogoliubov modes, obtained from:

$$\begin{aligned} \mathcal{L}_j^d f_n^j + J(f_n^{j+1} + f_n^{j-1}) - c_j^2 U h_n^j &= \epsilon_j f_n^j \\ \mathcal{L}_j^d h_n^j + J(h_n^{j+1} + h_n^{j-1}) - c_j^{*2} U f_n^j &= -\epsilon_j h_n^j, \end{aligned} \quad (\text{A4})$$

where  $\mathcal{L}_j^d \equiv 2n_j U + \nu_j - \mu$  and  $f_n^j \equiv f_n(jd)$ .

The expression for the fluctuations  $\delta\hat{b}_j$  in Eq. (A3) may be inverted by using the relation:

$$\sum_j [f_n(jd)f_m^*(jd) - h_n(jd)h_m^*(jd)] = \delta_{mn}, \quad (\text{A5})$$

in order to obtain  $\hat{\chi}_n$ :

$$\hat{\chi}_n = \sum_j [f_n(jd)\delta\hat{b}_j + h_n(jd)\delta\hat{b}_j^\dagger]. \quad (\text{A6})$$

In Section III C 4 we use this expression to evaluate the occupation numbers

$$\bar{n}_k = \langle \hat{\chi}_k^\dagger \hat{\chi}_k \rangle \quad (\text{A7})$$

of the low energy quasiparticle modes in the lattice in the TWA simulations by substituting  $\delta\hat{b}_j = \hat{b}_j - c_j$ , so that  $\bar{n}_k$  is obtained from the numerically evaluated correlation functions involving  $\hat{b}_j$ 's.

The atom number operator  $\hat{n}_i$  at the site  $i$  may be obtained by noting that we may expand to first order in  $\delta\hat{b}_i$ :  $\hat{b}_i^\dagger \hat{b}_i \simeq n_i + \hat{n}_i$ , for

$$\hat{n}_i = \sqrt{\bar{n}_i} \sum_j (w_j \hat{\chi}_j + w_j^* \hat{\chi}_j^\dagger), \quad (\text{A8})$$

where  $w_j \equiv f_j - h_j$ . Moreover, we introduce the phase operator at the site  $i$  as

$$\hat{\varphi}_i = -\frac{i}{2\sqrt{\bar{n}_i}} \sum_j (r_j \hat{\chi}_j - r_j^* \hat{\chi}_j^\dagger), \quad (\text{A9})$$

for which the commutator  $[\hat{n}_j, \hat{\varphi}_j] = i$  and we have defined  $r_j \equiv f_j + h_j$ .

Diagonalizing Eqs. (A4) yields the results for the number fluctuations in the  $i$ th site and the phase fluctuations between the  $k$ th and  $l$ th site:

$$(\Delta n_i)^2 = n_i \sum_j |w_j|^2 (2\bar{n}_j + 1), \quad (\text{A10})$$

and

$$\begin{aligned} (\Delta \varphi_{kl})^2 &\equiv ((\hat{\varphi}_k - \hat{\varphi}_l)^2) \\ &= \frac{1}{4} \sum_j \left| \frac{r_j(kd)}{\sqrt{\bar{n}_k}} - \frac{r_j(ld)}{\sqrt{\bar{n}_l}} \right|^2 (2\bar{n}_j + 1), \end{aligned} \quad (\text{A11})$$

where  $\bar{n}_j = \langle \hat{\chi}_j^\dagger \hat{\chi}_j \rangle$  is the thermal population of the  $j$ th phonon mode in the lattice.

In an inhomogeneous BEC, the phonon modes are spatially localized and Eqs. (A10) and (A11) generally lead to spatially varying density and phase fluctuations. However, in the homogeneous case ( $\nu_i = 0$ ) the Bogoliubov expressions for the phase and number fluctuations are

suitable for an analytic treatment. In the case of the homogeneous system with  $n$  atoms per site, we obtain the excitation frequencies [60, 61]:

$$(\hbar\omega_q)^2 = 4J \sin^2 \left( \frac{qd}{2} \right) \left[ 4J \sin^2 \left( \frac{qd}{2} \right) + 2nU \right], \quad (\text{A12})$$

where  $q$  is the quasiparticle momentum with periodic boundary conditions, so that  $qd = 2\pi m/N_p$ , for  $m = -N_p/2, \dots, N_p/2 - 1$ , and  $N_p$  denotes the number of lattice sites. Moreover, in the experimentally interesting regime  $nU \gg J$  we obtain

$$\hbar\omega_q \simeq 2\sqrt{2nJU} |\sin(qd/2)|, \quad (\text{A13})$$

and for  $N_p \gg 1$  the lowest phonon mode energy

$$\hbar\omega_{q,\min} \simeq \frac{2\pi\sqrt{2nJU}}{N_p}. \quad (\text{A14})$$

Moreover, in the limit  $nU \gg J$ , the expressions for the number and phase fluctuations in Eqs. (A10) and (A11) can be approximated by [60, 61]:

$$(\Delta n_i)^2 \simeq \sum_q \frac{\hbar\omega_q}{2UN_p} (2\bar{n}_q + 1), \quad (\text{A15})$$

$$(\Delta \varphi_{i,i+1})^2 \simeq \sum_q \frac{\hbar\omega_q}{4nJN_p} (2\bar{n}_q + 1), \quad (\text{A16})$$

where  $\bar{n}_q$  is the occupation number of the phonon mode with the quasimomentum  $q$ . By replacing the sum by an integral when  $N_p$  is large, these yield at  $T = 0$ :

$$(\Delta n_i)^2 \simeq \frac{1}{\pi} \left( \frac{8nJ}{U} \right)^{1/2}, \quad (\text{A17})$$

$$(\Delta \varphi_{i,i+1})^2 \simeq \frac{1}{2} \left( \frac{2U}{nJ} \right)^{1/2}. \quad (\text{A18})$$

Formulas (A17) and (A18) provide useful comparisons to our numerical results.

In Fig. 14 we show the numerical results of the number and phase fluctuations in a harmonic trap, obtained by solving the Bogoliubov approximation to the BHH from Eqs. (A4) for a typical system in our simulations. We evaluate  $\Delta n_0$  using Eq. (A10) and compare it to the homogeneous results with  $n = n_0$ , determined by Eq. (A17). We also calculate  $(\Delta \varphi_{0,i})^2$  as a function of the lattice height  $s$  using Eq. (A11) for several sites along the lattice and we evaluate  $(\Delta \varphi_{0,1})^2$  in the homogeneous case from Eq. (A18). The inhomogeneous results for the phase fluctuations are numerically very unstable due to the summation formula in Eq. (A11) and spatially localized phonon modes. Consequently, the results for  $(\Delta \varphi_{0,i})^2$  should only be considered as an order of magnitude estimates, describing the qualitative behavior. Numerically we find the Bogoliubov result in a harmonic trap for  $\Delta n_0$  to be larger and for  $\Delta \varphi_{01}$  smaller than the homogeneous result. The harmonic trap significantly reduces phase fluctuations close to the trap center and enhance them close to the edge of the atom cloud.

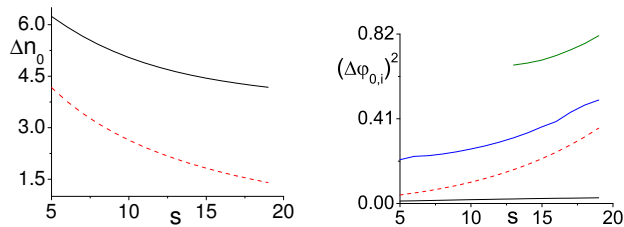


FIG. 14: The number and phase fluctuations of atoms in a combined harmonic trap and optical lattice, obtained by numerically solving the Bogoliubov modes in the discrete tight-binding approximation. On left we show  $\Delta n_0$  for various values of  $s$  (solid line) and the analytic homogenous result with  $n = n_0$  in Eq. (A17) (dashed line). Here the total atom number  $N_0 = 2000$ , the nonlinear constant  $g_{1D} = 0.05\hbar\omega l$ ,  $T = 0$ , and  $n_0 \simeq 80$ -90 atoms. On right for the same inhomogeneous system we show approximate  $(\Delta\varphi_{0,i})^2$  for  $i = 1, 13, 16$  (solid lines from bottom) and the analytic homogeneous result for  $(\Delta\varphi_{0,1})^2$  (dashed line) from Eq. (A18). The inhomogeneous results for  $(\Delta\varphi_{0,i})^2$  should only be understood qualitatively as an order of magnitude estimates.

## APPENDIX B: THREE-BODY LOSSES

The TWA approach in this paper ignored any atom losses due to three-body collisions. The TWA with incorporated three-body losses would result in a dynamical stochastic noise term in Eq. (5) and more demanding numerics. We may estimate the importance of the three-body losses in an optical lattice system as in Ref. [71]. In a deep lattice with a fragmented condensate the atom

loss rate at the central lattice site (with  $n_0 \gg 1$ ) is approximately

$$\frac{dn_0}{dt} \simeq -\Gamma n_0^3, \quad \Gamma = \frac{K_3}{12} \int d^3r |\eta_0(\mathbf{r})|^6, \quad (\text{B1})$$

where  $K_3$  is the recombination event rate and  $\eta_0(\mathbf{r})$  is the ground state wave function in the central site with the atom number  $n_0$ . For simplicity, we have ignored the correlations between different lattice sites.

We obtain from Eq. (B1):

$$\Gamma \simeq \frac{K_3 \sqrt{s}}{144 \sqrt{3} \pi a^2 d^2 l^2} \left( \frac{g_{1D}}{\hbar \omega l} \right)^2 \simeq \frac{67 K_3}{a^2 l^4}. \quad (\text{B2})$$

Here on the right-hand side we have introduced the same parameters as in Fig. 6 with  $s = 20$ . In order to the three-body loss rate to be negligible over the time scale of the simulations we require  $\Gamma n_0^3 \ll \omega$  that may be satisfied for sufficiently large  $l$ . For the 1D description of the dynamics to be valid we also need to maintain  $\hbar\omega_\perp \gtrsim nU \sim n g_{1D} k s^{1/4} / \sqrt{2\pi}$ . For example, for  $^{87}\text{Rb}$  we use  $K_3 \simeq 2.2 \times 10^{-28} \text{ cm}^6/\text{s}$  [72] and  $a \simeq 5.313 \text{ nm}$ . Then  $\omega = 2\pi \times 1 \text{ Hz}$  yields  $\Gamma n_0^3 \simeq 0.006\omega$  and, using an average occupation number  $n$ ,  $\hbar\omega_\perp \sim 3n g_{1D} k s^{1/4} / \sqrt{2\pi}$  with  $\omega_\perp \gg \omega$ . The effect of the three-body losses could be further reduced by using different atoms and the Feshbach resonances.

## ACKNOWLEDGMENTS

We acknowledge financial support from the EPSRC.

- 
- [1] B.P. Anderson and M.A. Kasevich, *Science* **282**, 1686 (1998).
  - [2] M. Greiner, I. Bloch, O. Mandel, T.W. Hänsch, and T. Esslinger, *Phys. Rev. Lett.* **87**, 160405 (2001).
  - [3] M. Greiner, O. Mandel, T.W. Hänsch, and I. Bloch, *Nature* **419**, 51 (2002).
  - [4] Z. Hadzibabic, S. Stock, B. Battelier, V. Bretin, and J. Dalibard, *Phys. Rev. Lett.* **93**, 180403 (2004).
  - [5] A.K. Tuchman, C. Orzel, A. Polkovnikov, and M.A. Kasevich, *cond-mat/0504762*.
  - [6] C. Orzel, A.K. Tuchman, M.L. Fenselau, M. Yasuda, and M.A. Kasevich, *Science* **291**, 2386 (2001).
  - [7] M. Greiner, O. Mandel, T. Esslinger, T.W. Hänsch, and I. Bloch, *Nature* **415**, 39 (2002).
  - [8] T. Stöferle, H. Moritz, C. Schori, M. Köhl, and T. Esslinger, *Phys. Rev. Lett.* **92**, 130403 (2004).
  - [9] B. Paredes, A. Widera, V. Murg, O. Mandel, S. Fölling, I. Cirac, G.V. Shlyapnikov, T.W. Hänsch, and I. Bloch, *Nature* **429**, 277 (2004).
  - [10] K. Xu, Y. Liu, J.R. Abo-Shaeer, T. Mukaiyama, J.K. Chin, D.E. Miller, W. Ketterle, K.M. Jones, and E. Tiesinga, *Phys. Rev. A* **72**, 043604 (2005).
  - [11] C.D. Fertig, K.M. O'Hara, J.H. Huckans, S.L. Rolston, W.D. Phillips, and J.V. Porto, *Phys. Rev. Lett.* **94**, 120403 (2005).
  - [12] S. Burger, F.S. Cataliotti, C. Fort, F. Minardi, M. Inguscio, M.L. Chiofalo, and M.P. Tosi *Phys. Rev. Lett.* **86**, 4447 (2001).
  - [13] O. Morsch, J.H. Müller, M. Cristiani, D. Ciampini, and E. Arimondo, *Phys. Rev. Lett.* **87**, 140402 (2001).
  - [14] L. Fallani, L. De Sarlo, J.E. Lye, M. Modugno, R. Saers, C. Fort, and M. Inguscio, *Phys. Rev. Lett.* **93**, 140406 (2004).
  - [15] L. De Sarlo, L. Fallani, J.E. Lye, M. Modugno, R. Saers, C. Fort, and M. Inguscio, *Phys. Rev. A* **72**, 013603 (2005).
  - [16] G. Modugno, F. Ferlaino, R. Heidemann, G. Roati, and M. Inguscio, *Phys. Rev. A* **68**, 011601(R) (2003).
  - [17] M. Köhl, H. Moritz, T. Stöferle, K. Günter, and T. Esslinger, *Phys. Rev. Lett.* **94**, 080403 (2005).
  - [18] J.K. Chin, D.E. Miller, Y. Liu, C. Stan, W. Setiawan, C. Sanner, K. Xu, and W. Ketterle, *cond-mat/0607298*.
  - [19] D. Jaksch and P. Zoller, *Ann. of Phys.* **315**, 52 (2005).
  - [20] T. Gericke, F. Gerbier, A. Widera, S. Fölling, O. Mandel, and I. Bloch, *cond-mat/0603590*.
  - [21] L. Santos, M.A. Baranov, J.I. Cirac, H.-U. Everts, H. Fehrmann, and M. Lewenstein, *Phys. Rev. Lett.* **93**, 030601 (2004).

- [22] A. Sanpera, A. Kantian, L. Sanchez-Palencia, J. Zakrzewski, and M. Lewenstein, Phys. Rev. Lett. **93**, 040401 (2004).
- [23] H.P. Büchler, M. Hermele, S.D. Huber, M.P.A. Fisher, and P. Zoller, Phys. Rev. Lett. **95**, 040402 (2005).
- [24] J. Ruostekoski, G.V. Dunne, and J. Javanainen, Phys. Rev. Lett. **88**, 180401 (2002).
- [25] R. Roth and K. Burnett, J. Opt. B **5**, S50 (2003).
- [26] D. Jaksch and P. Zoller, New J. Phys. **5**, 56 (2003).
- [27] J.K. Pachos and E. Rico, Phys. Rev. A **70**, 053620 (2004).
- [28] J. Javanainen and J. Ruostekoski, Phys. Rev. Lett. **91**, 150404 (2003).
- [29] K. Osterloh, M. Baig, L. Santos, P. Zoller, and M. Lewenstein, Phys. Rev. Lett. **95**, 010403 (2005).
- [30] L. Isella and J. Ruostekoski, Phys. Rev. A **72**, 011601(R) (2005).
- [31] Y.B. Band and M. Trippenbach, Phys. Rev. A **65**, 053602 (2002).
- [32] S.B. McKagan, D.L. Feder, and W.P. Reinhardt, Phys. Rev. A **74**, 013612 (2006).
- [33] M.J. Holland and K. Burnett, Phys. Rev. Lett. **71**, 1355 (1993).
- [34] P.D. Drummond and A.D. Hardman, Europhys. Lett. **21**, 279 (1993).
- [35] J.F. Corney and P.D. Drummond, J. Opt. Soc. Am. B **18**, 139 (2001).
- [36] M.J. Steel, M.K. Olsen, L.I. Plimak, P.D. Drummond, S.M. Tan, M.J. Collett, D.F. Walls, and R. Graham, Phys. Rev. A **58**, 4824 (1998).
- [37] A. Sinatra, C. Lobo, and Y. Castin, Phys. Rev. Lett. **87**, 210404 (2001).
- [38] A. Sinatra, C. Lobo, and Y. Castin, J. Phys. B **35**, 3599 (2002).
- [39] C.W. Gardiner, J.R. Anglin, and T.I.A. Fudge, J. Phys. B **35**, 1555 (2002).
- [40] K. Góral, M. Gajda, and K. Rzażewski, Phys. Rev. A **66**, 051602(R) (2002).
- [41] A. Polkovnikov, Phys. Rev. A **68**, 033609 (2003).
- [42] A. Polkovnikov and D.W. Wang, Phys. Rev. Lett. **93**, 070401 (2004).
- [43] J. Ruostekoski and L. Isella, Phys. Rev. Lett. **95**, 110403 (2005).
- [44] M.J. Davis, S.A. Morgan, and K. Burnett, Phys. Rev. Lett. **87**, 160402 (2001); Phys. Rev. A **66**, 053618 (2002).
- [45] R.A. Duine and H.T.C. Stoof, Phys. Rev. A **65**, 013603 (2002).
- [46] B.J. Dabrowska-Wüster, S. Wüster, A.S. Bradley, M.J. Davis, and E.A. Ostrovskaya, cond-mat/0607332.
- [47] D.F. Walls and G.J. Millburn, *Quantum Optics*, (Springer, New York, 1994).
- [48] C.W. Gardiner and P. Zoller, *Quantum Noise* (Springer, Berlin, 1999).
- [49] K.M. O'Hara, S.R. Granade, M.E. Gehm, T.A. Savard, S. Bali, C. Freed, and J.E. Thomas, Phys. Rev. Lett. **82**, 4204 (1999).
- [50] K.V. Kheruntsyan, D.M. Gangardt, P.D. Drummond, and G.V. Shlyapnikov, Phys. Rev. Lett. **91**, 040403 (2003).
- [51] J. Javanainen and J. Ruostekoski, J. Phys. A: Math. Gen. **39**, L179 (2006).
- [52] A.J. Leggett and F. Sols, Found. Phys. **21**, 353 (1991).
- [53] J. Javanainen and M.Y. Ivanov, Phys. Rev. A **60**, 2351 (1999).
- [54] J. Ruostekoski and D. F. Walls, Phys. Rev. A **58**, R50 (1998).
- [55] I. Zapata, F. Sols, and A.J. Leggett, Phys. Rev. A **67**, 021603(R) (2003).
- [56] R. Gati, B. Hemmerling, J. Fölling, M. Albiez, and M.K. Oberthaler, Phys. Rev. Lett. **96**, 130404 (2006).
- [57] M.R. Andrews, C.G. Townsend, H.J. Miesner, D.S. Durfee, D.M. Kurn, and W. Ketterle, Science **275**, 637 (1997).
- [58] K. Mølmer, Phys. Rev. A **58**, 566 (1998).
- [59] A.I. Streltsov, L.S. Cederbaum, and N. Moiseyev, Phys. Rev. A **70**, 053607 (2004).
- [60] J. Javanainen, Phys. Rev. A **60**, 4902 (1999).
- [61] K. Burnett, M. Edwards, C.W. Clark, and M. Shotton, J. Phys. B **35**, 1671 (2002).
- [62] The excitations of collective modes due to nonadiabatic splitting was addressed by: J. Plata, Phys. Rev. A **69**, 033604 (2004).
- [63] P.B. Blakie and J.V. Porto, Phys. Rev. A **69**, 013603 (2004).
- [64] S. Burger, F.S. Cataliotti, C. Fort, P. Maddaloni, F. Minardi, and M. Inguscio, Europhys. Lett. **57**, 1 (2002).
- [65] In the studied 1D system we never observed any considerable rethermalization on the time scale of our simulations. This is quite different from the TWA simulations in 3D [38] and may be the consequence of the smaller density of states in 1D.
- [66] L.I. Plimak, M.K. Olsen, M. Fleischhauer, and M.J. Collett, Europhys. Lett. **56**, 372 (2001).
- [67] J. Ruostekoski and J.R. Anglin, Phys. Rev. Lett. **86**, 3934 (2001).
- [68] D. Jaksch, C. Bruder, J.I. Cirac, C.W. Gardiner, and P. Zoller, Phys. Rev. Lett. **81**, 3108 (1998).
- [69] M.P.A. Fisher, P.B. Weichman, G. Grinstein, and D.S. Fisher, Phys. Rev. B **40**, 546 (1989).
- [70] W. Zwerger, J. Opt. B: Quant. Semiclass. Opt. **5**, S9 (2003).
- [71] M.W. Jack and M. Yamashita, Phys. Rev. A **67**, 033605 (2003).
- [72] J. Söding, D. Guéry-Odelin, P. Desbiolles, F. Chevy, H. Inamori, and J. Dalibard, Appl. Phys. B: Lasers Opt. **B69**, 257 (1999).